


Universal relationship between low-energy antiferromagnetic fluctuations and superconductivity in $\text{BaFe}_2(\text{As}_{1-x}\text{P}_x)_2$

Shunsaku Kitagawa,^{1,*} Takeshi Kawamura,¹ Kenji Ishida,¹ Yuta Mizukami,² Shigeru Kasahara,¹ Takasada Shibauchi,² Takahito Terashima,¹ and Yuji Matsuda¹

¹*Department of Physics, Kyoto University, Kyoto 606-8502, Japan*

²*Department of Advanced Materials Science, University of Tokyo, Kashiwa, Chiba 277-8561, Japan*

 (Received 12 March 2019; revised manuscript received 28 July 2019; published 12 August 2019)

To identify the key parameter for optimal superconductivity in iron pnictides, we measured the ^{31}P -NMR relaxation rate on $\text{BaFe}_2(\text{As}_{1-x}\text{P}_x)_2$ ($x = 0.22$ and 0.28) under pressure and compared the effects of chemical substitution and physical pressure. For $x = 0.22$, structural and antiferromagnetic (AFM) transition temperatures both show minimal changes with pressure up to 2.4 GPa, whereas the superconducting transition temperature T_c increases to twice its former value. In contrast, for $x = 0.28$ near the AFM quantum critical point (QCP), the structural phase transition is quickly suppressed by pressure and T_c reaches a maximum. The analysis of the temperature-dependent nuclear relaxation rate indicates that these contrasting behaviors can be quantitatively explained by a single curve of the T_c dome as a function of Weiss temperature θ , which measures the distance to the QCP. Moreover, the T_c - θ curve under pressure precisely coincides with that with a chemical substitution, which is indicative of the existence of a universal relationship between low-energy AFM fluctuations and superconductivity on $\text{BaFe}_2(\text{As}_{1-x}\text{P}_x)_2$.

DOI: [10.1103/PhysRevB.100.060503](https://doi.org/10.1103/PhysRevB.100.060503)

Identifying the key parameter that determines the optimal superconducting transition temperature (T_c) in superconducting phase diagrams involving other electronic orders is of primary importance to understand the mechanism of superconductivity. In the Bardeen-Cooper-Schrieffer (BCS) theory, T_c at the weak-coupling limit is expressed as [1]

$$T_c = \frac{1.13\hbar\omega_D}{k_B} \exp\left(-\frac{1}{N(0)V}\right), \quad (1)$$

where ω_D is the Debye frequency, k_B is Boltzmann's constant, $N(0)$ is the density of states at the Fermi energy, and V is the pairing electron-phonon interaction. Therefore, it is well known that the T_c of a BCS superconductor is affected by the isotope's mass and pressure, both of which change ω_D and/or $N(0)$. On the other hand, in materials that exhibit superconductivity in the vicinity of the antiferromagnetic (AFM) order, such as cuprates, iron pnictides, and heavy-fermion superconductors, it has been pointed out that T_c is roughly proportional to the characteristic energy of spin fluctuations based on self-consistent renormalization (SCR) theory [2–4], suggesting that these superconductors are mediated by AFM fluctuations. However, it is not straightforward to find the most significant parameter for optimizing T_c even in these superconductors because pressure and chemical substitutions, which are general methods to tune the Néel temperature T_N , and T_c , also change several physical quantities in these superconductors.

$\text{BaFe}_2(\text{As}_{1-x}\text{P}_x)_2$, which has a tetragonal ThCr_2Si_2 -type structure with space group $I4/mmm$ (D_{4h}^{17} , No. 139), is a

member of the iron-based superconductors. $\text{BaFe}_2(\text{As}_{1-x}\text{P}_x)_2$ is known to be one of the best compounds for investigations among the iron-based superconductors, because superconductivity is induced by the isovalence substitution of P; furthermore, clean single crystals, in which the quantum oscillations are observable, are obtained. Figure 1 shows the x - T phase diagram of $\text{BaFe}_2(\text{As}_{1-x}\text{P}_x)_2$ as a function of the concentration of P at ambient pressure [5]. The resistivity, nuclear magnetic resonance (NMR), and penetration depth measurements indicate that an AFM quantum critical point (QCP) is located at $x \sim 0.3$, and T_c reaches a maximum near the QCP [5,6]. According to SCR theory, in the case of a two-dimensional AFM metal, the distance from the QCP can be determined from the Weiss temperature θ , evaluated by fitting the nuclear spin-lattice relaxation rate divided by temperature $1/T_1T$ to the Curie-Weiss formula [7],

$$\frac{1}{T_1T} = a + \frac{b}{T + \theta}, \quad (2)$$

where a originates from the intraband contributions related to the density of states, and b is related to the strength of AFM fluctuations, thus $-\theta$ is regarded as the temperature at which the AFM correlations diverge, i.e., the AFM ordering temperature. The sign of θ is changed by varying the P substitution and θ becomes zero at $x \sim 0.3$, indicating the existence of an AFM QCP. A similar relationship between superconductivity and AFM QCP was observed in other “122” systems [8–11]. In addition, ac susceptibility measurements on $\text{BaFe}_2(\text{As}_{1-x}\text{P}_x)_2$ under pressure revealed that the pressure dependence of T_c has a dome shape similar to the isovalent P substitution phase diagram at ambient pressure [12]. However, the extent to which AFM fluctuations are changed by

*kitagawa.shunsaku.8u@kyoto-u.ac.jp

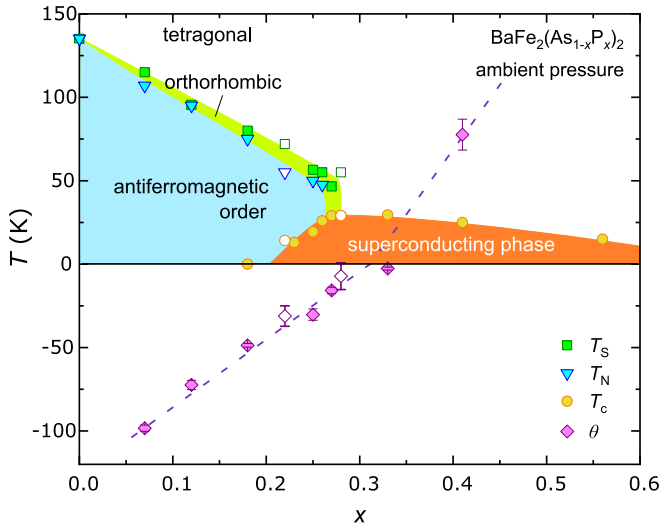


FIG. 1. P concentration x - T phase diagram of $\text{BaFe}(\text{As}_{1-x}\text{P}_x)_2$ at ambient pressure [5]. Squares, triangles, circles, and diamonds represent the structural phase transition temperature T_S , Néel temperature T_N , superconducting transition temperature T_c , and the Weiss temperature θ , respectively. The open symbols indicate the data from the samples in this study. The dashed line is intended to guide the eye.

pressure and the relationship between AFM fluctuations and superconductivity as a result of the changing pressure has not yet been reported. In general, an isovalent substitution does not always give the same effect as an applying pressure, e.g., phase diagrams are quite different between $\text{Fe}(\text{Se}_{1-x}\text{S}_x)$ [13] and pressurized FeSe [14] as well as between $\text{Ce}(\text{Ir}_{1-x}\text{Rh}_x)\text{In}_5$ and pressurized CeIrIn_5 [15]. In $\text{BaFe}_2(\text{As}_{1-x}\text{P}_x)_2$, the tuning parameter dependence of structural parameters such as lattice constants are different on P substitution [16] and under pressure [17]. Therefore, the effect of these parameters for superconductivity and AFM fluctuations might be different, although both parameters induce superconductivity [16,18]. To date, orbital fluctuations have also been considered to play an important role for the pairing interaction in iron-pnictide superconductors [19], and in general it is difficult to measure one of these fluctuations separately. For this purpose, we would like to point out that ^{31}P -NMR is one of the best techniques to probe the AFM fluctuations solely, because the nuclear spin of ^{31}P is $1/2$ and electric coupling with the lattice is entirely absent.

In this Rapid Communication, we performed ^{31}P -NMR measurements on single-crystal $\text{BaFe}_2(\text{As}_{1-x}\text{P}_x)_2$ ($x = 0.22$ and 0.28) under pressure to investigate the effect of pressure on the magnetic properties and the phase diagram. At $x = 0.22$, the structural phase transition temperatures $T_S = 72$ K and $T_N = 55$ K are little changed by increasing the pressure up to 2.4 GPa, whereas T_c is increased to twice the original value. On the other hand, for $x = 0.28$, $T_S = 55$ K is quickly suppressed by pressure and T_c decreases gradually with increasing pressure. From a nuclear relaxation rate analysis, we find that the dependence of T_c on the Weiss temperature θ can be quantitatively scaled between pressure and P-content variations, indicating the universal relationship

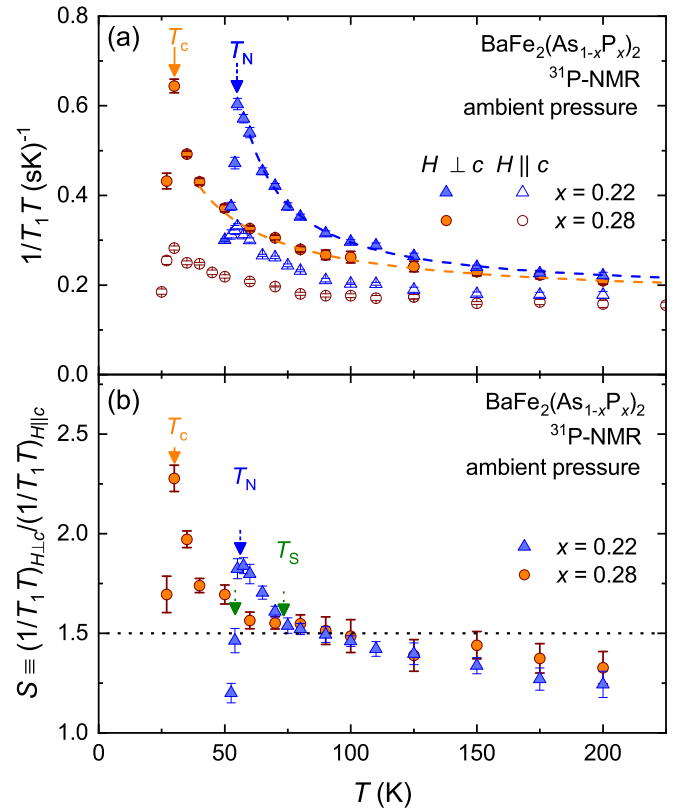


FIG. 2. (a) Temperature dependence of $1/T_1T$ for $H \parallel c$ and $H \perp c$, and (b) the ratio of $1/T_1T$, $S \equiv (1/T_1T)_{H \perp c} / (1/T_1T)_{H \parallel c}$, at ambient pressure measured for the $x = 0.22$ and $x = 0.28$ samples. The dashed lines of (a) are fitting curves by the Curie-Weiss formula. The dotted line of (b) indicates the value of 1.5.

between low-energy AFM fluctuations and superconductivity in $\text{BaFe}_2(\text{As}_{1-x}\text{P}_x)_2$.

Single crystals of $\text{BaFe}_2(\text{As}_{1-x}\text{P}_x)_2$ were prepared as described elsewhere [16]. $T_c = 14.1$ K for $x = 0.22$ and 29.1 K for $x = 0.28$ were determined by ac susceptibility measurements using an NMR coil. Pressure was generated in a piston cylinder-type pressure cell with Daphne 7373 for the $x = 0.22$ samples, and an indenter-type pressure cell with Daphne 7474 for the $x = 0.28$ samples [20,21]. The applied pressure P was determined from T_c of the lead manometer by using the relation of $P(\text{GPa}) = [T_c(0) - T_c(P)](\text{K}) / 0.364(\text{K/GPa})$ [22,23]. The ^{31}P (nuclear spin $I = 1/2$, nuclear gyromagnetic ratio $^{31}\gamma_N / 2\pi = 17.237$ MHz/T, and natural abundance 100%) nuclear spin-lattice relaxation rate $1/T_1$ was determined by fitting the time variation of the spin-echo intensity after the saturation of the nuclear magnetization to a single exponential function across the entire temperature range as shown in Fig. S1 [24].

Figure 2(a) shows the temperature dependence of $1/T_1T$ for $H \parallel c$ and $H \perp c$, and Fig. 2(b) the ratio of $1/T_1T$ anisotropy, $S \equiv (1/T_1T)_{H \perp c} / (1/T_1T)_{H \parallel c}$, at $x = 0.22$ and $x = 0.28$ at ambient pressure. As a result of strong AFM fluctuations, $1/T_1T$ is enhanced toward T_N and T_c with decreasing T ; $1/T_1T$ shows a peak at T_N by critically slowing down in the $x = 0.22$ sample, and $1/T_1T$ decreases below T_c due to the opening of the superconducting gap in the $x = 0.28$ sample.

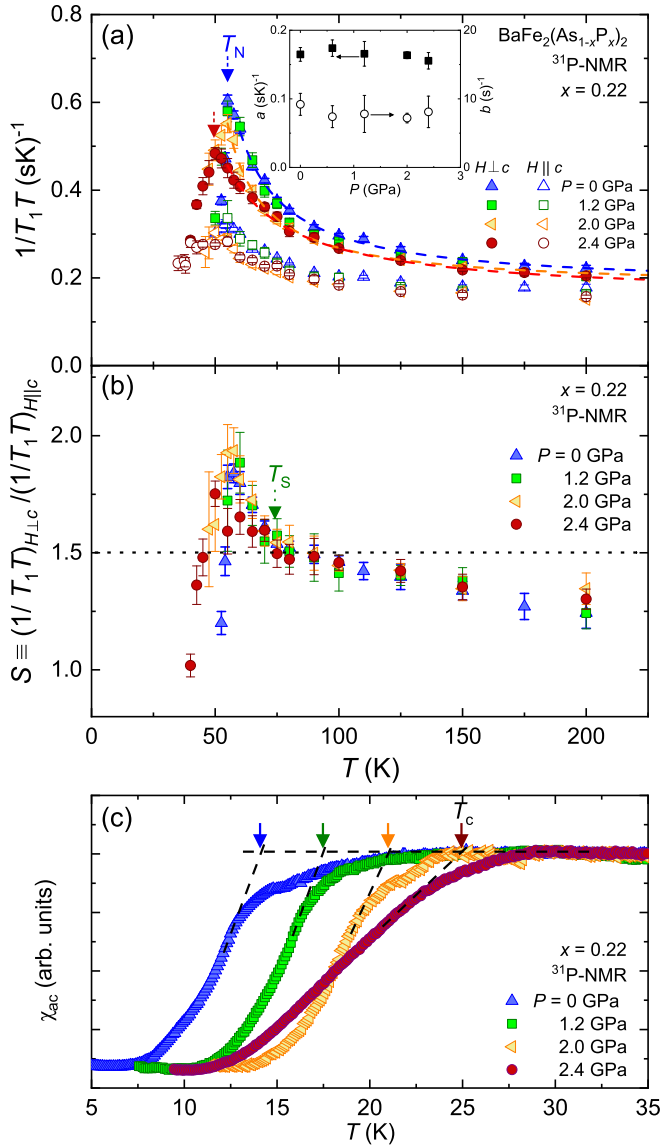


FIG. 3. (a) Temperature dependence of $1/T_1T$ for $H \parallel c$ and $H \perp c$, (b) the ratio of $1/T_1T$, and (c) ac susceptibility for $x = 0.22$ under pressure. The dashed lines of (a) are fitting curves by the Curie-Weiss formula. The dotted line of (b) indicates the value of 1.5. The dashed lines of (c) are intended to guide the eye.

Below T_N and T_c , the intensity of the NMR signal of the two samples weakens to an extent that $1/T_1T$ could not be measured accurately. The temperature dependence of $1/T_1T$ for $H \perp c$ is consistent with the previous report measured in the mosaic of single crystals [5]. The anisotropy ratio S of $1/T_1T$ is ~ 1.25 at high temperatures in both samples, which originates from the stripe-type spin correlations. As reported previously [25–27], the anisotropy ratio of $1/T_1T$ in the system dominated by stripe correlations can be written as

$$S \equiv \frac{(1/T_1T)_{H \perp c}}{(1/T_1T)_{H \parallel c}} = \left| \frac{S_a(\omega_{\text{res}})}{S_c(\omega_{\text{res}})} \right|^2 + \frac{1}{2}, \quad (3)$$

where $(1/T_1T)_{H \perp c} = \frac{(1/T_1T)_{H \parallel a} + (1/T_1T)_{H \parallel b}}{2}$ and $S_i(\omega)$ ($i = a$ and c) denotes the spin fluctuations along the i axis probed by

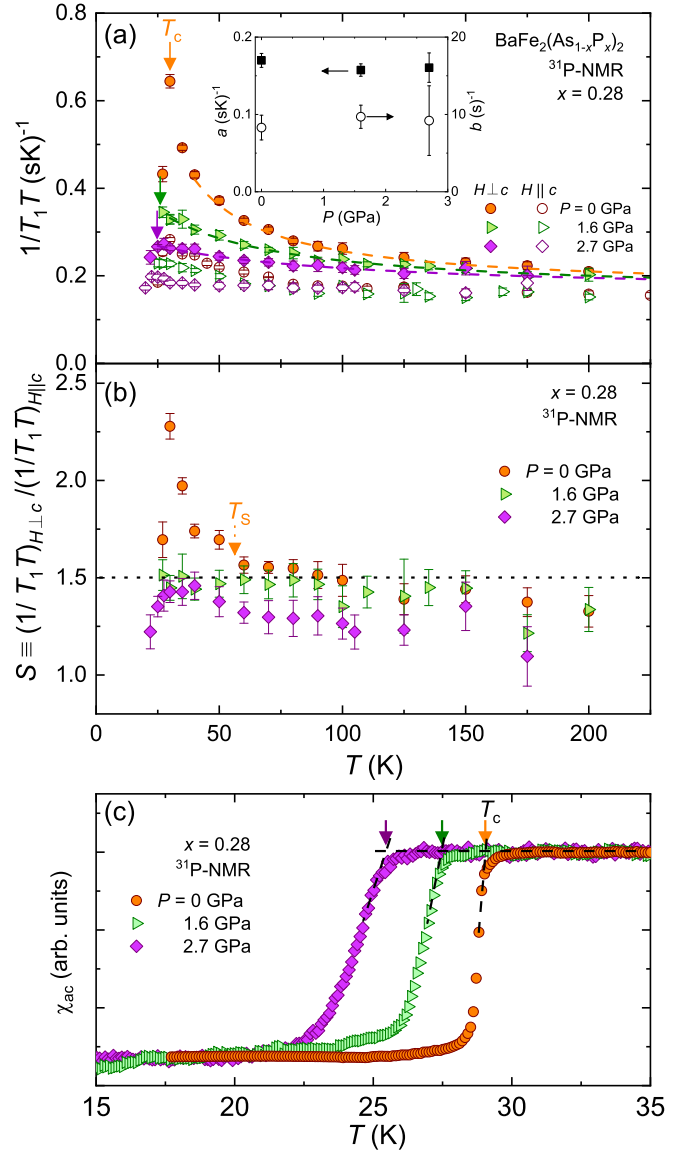


FIG. 4. (a) Temperature dependence of $1/T_1T$ for $H \parallel c$ and $H \perp c$, (b) the ratio of $1/T_1T$, and (c) ac susceptibility at $x = 0.28$ under pressure. The dashed lines of (a) are fitting curves by the Curie-Weiss formula. The dotted line of (b) indicates the value of 1.5. The dashed lines of (c) are intended to guide the eye.

NMR frequency ω_{res} . Therefore, S becomes 1.5 if the Fe spin fluctuations are isotropic ($|S_a| = |S_c|$) with the stripe correlations, whereas the ratio becomes higher than 1.5 if in-plane stripe fluctuations develop ($|S_a| > |S_c|$). In various iron-based superconductors, a ratio of ~ 1.5 , suggesting the presence of a stripe AFM correlation, has been observed just above T_S or T_c [25–29]. Note that S is smaller than 1.5 at high temperatures, originating from the existence of a paramagnetic contribution. On cooling, S increases more rapidly below $\sim T_S$, indicating that the in-plane Fe spin fluctuations increase below the structural phase transition. The breaking of in-plane fourfold symmetry enhances the stripe-type AFM correlations, because the direction of the AFM correlations is determined. In fact, the same enhancement of S below T_S was clearly observed in $\text{LaFeAs}(\text{O}_{1-x}\text{F}_x)$ [27]. We defined

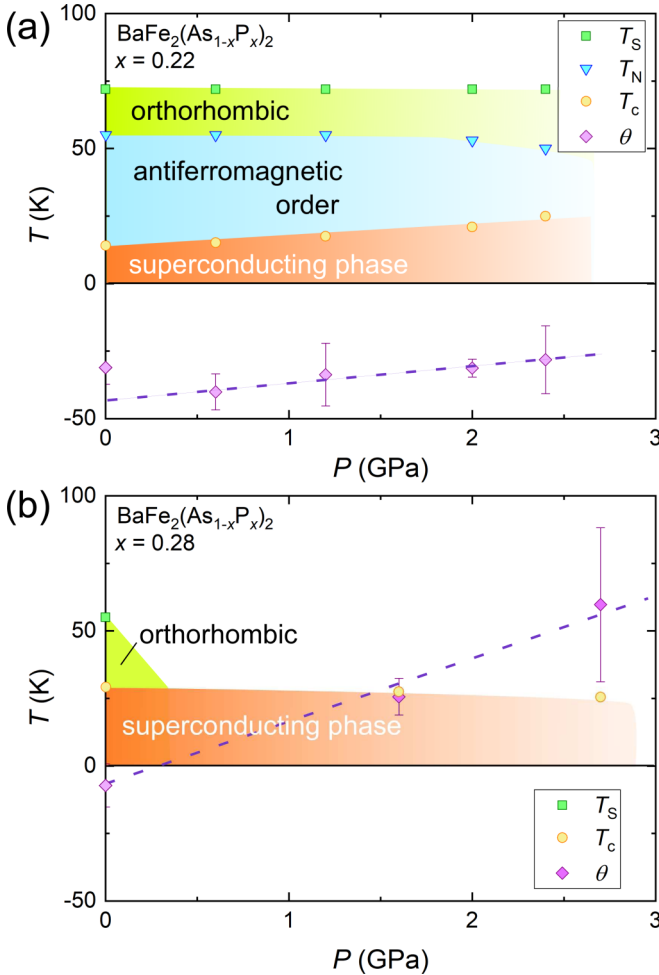


FIG. 5. P - T phase diagram at (a) $x = 0.22$ and (b) $x = 0.28$. The dashed lines are provided to guide the eye.

the structural-transition temperature T_S as the onset of the increase in S and determined the AFM ordering temperature T_N as the peak of $1/T_1T$.

The pressure dependence of T_N , T_S , and T_c was investigated with ^{31}P -NMR and ac susceptibility measurements. Figure 3(a) shows the temperature dependence of $1/T_1T$ for $H \parallel c$ and $H \perp c$, Fig. 3(b) for S , and Fig. 3(c) the ac susceptibility at $x = 0.22$ under pressure. Although T_c increases from 14.1 K at ambient pressure to 25.0 K at 2.4 GPa, T_N and T_S show only little changes by pressure. The limitations of the pressure cell prevented us from reaching the maximum of T_c . In contrast, $1/T_1T$ of the $x = 0.28$ sample is strongly affected by pressure, as shown in Fig. 4. The AFM fluctuations and T_S are significantly suppressed by pressure.

To estimate the pressure evolution of the Weiss temperature θ , the temperature dependence of $1/T_1T$ was fitted to Eq. (2). We used the data for $H \perp c$ to compare with the previous results because $1/T_1T$ for $H \perp c$ is determined with the in-plane AFM fluctuations [25]. The fitting parameters of a and b are hardly changed by pressure, as shown in the insets of Figs. 3 and 4. This indicates that the pressure does not change the density of states, which is consistent with the band-structure calculation and the AFM-fluctuation component significantly [5]. We constructed the P - T phase diagrams of the $x = 0.22$

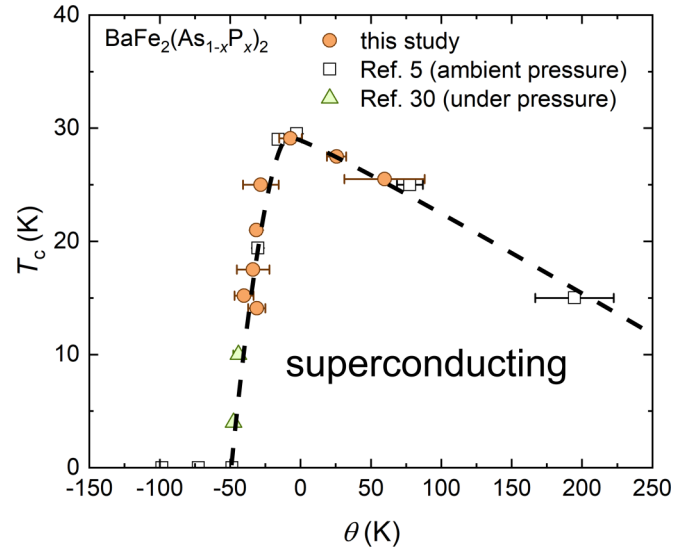


FIG. 6. θ dependence of T_c on $\text{BaFe}_2(\text{As}_{1-x}\text{P}_x)_2$ at ambient pressure [5] and under pressure. The dashed curve is added to guide the eye.

and 0.28 samples, as shown in Fig. 5. In the $x = 0.22$ sample, although T_N , T_S , and θ undergo small changes, the increase in T_c is large. In contrast, in the $x = 0.28$ sample, T_c gradually decreases with increasing pressure, although T_S is abruptly suppressed by pressure and θ largely increases from -7 K at ambient pressure to 60 K at 2.7 GPa, passing through the AFM QCP. To understand the relationship between the AFM critical fluctuations and superconductivity, T_c is plotted against θ obtained for both the P-substitution and pressure studies as shown in Fig. 6, where the previous results obtained in the mosaic single crystals of the $x = 0.20$ sample under pressure [30] were also analyzed by the same procedure for comparison. The dependence of T_c on magnetic fluctuations seems asymmetric before and after the AFM QCP, and this asymmetric behavior of T_c can be understood in terms of the presence of the AFM phase in the negative θ region, where the Fermi surfaces partially contribute to the AFM ordering. The dependence of T_c on θ obtained by tuning these two parameters is precisely consistent with each other, and this result strongly suggests the existence of a universal relationship between the low-energy AFM fluctuations and superconductivity in $\text{BaFe}_2(\text{As}_{1-x}\text{P}_x)_2$. Furthermore, we comment on the effect of the nematic fluctuations revealed by measuring $1/T_1$ of ^{75}As with nuclear quadrupole moment [31]. The nematic fluctuations were shown to be enhanced below approximately T_S and to possess inhomogeneous glassy dynamics [31]. As already mentioned, $1/T_1$ of the ^{31}P -NMR does not couple with the electric fluctuations related with the lattice dynamics, but only couples with magnetic fluctuations. In addition, the deviation from the Curie-Weiss behavior was observed even in $1/T_1T$ of ^{31}P below T_S , but the value of θ was evaluated from the temperature range above T_S , where the spin fluctuations are homogeneous. Thus, the θ we evaluated is related to the AFM fluctuations, which are not affected by the nematic fluctuations.

It is noteworthy that the phase diagram of $\text{BaFe}_2(\text{As}_{1-x}\text{P}_x)_2$ is well summarized by θ and that the T_c

maximum is observed near the AFM QCP even when the spin fluctuations are changed by pressure, indicating that the low-temperature properties are determined with the low-energy AFM fluctuations in the normal state, and that the maximum T_c near the AFM QCP is not accidental but an intrinsic property. Because the application of pressure introduces negligible disorder into the Fe plane and hardly changes the carrier content, and isovalent P substitution shows less significant disorder effects than that of Co or K substitution in BaFe_2As_2 , adjusting both of these parameters is an ideal way to change the strength of the electron correlations. A similar θ dependence of T_c was observed in various iron-based superconductors, although maximum T_c and the detailed θ dependence of T_c depend on the system [24].

In conclusion, we performed ^{31}P -NMR measurements on $\text{BaFe}_2(\text{As}_{1-x}\text{P}_x)_2$ ($x = 0.22$ and 0.28) under pressure to

investigate the relationship between low-energy AFM fluctuations and superconductivity. The pressure dependences of T_S , T_N , and T_c in these two samples are almost the same as the dependences of these temperatures of $\text{BaFe}_2(\text{As}_{1-x}\text{P}_x)_2$ on x at ambient pressure. This indicates the presence of a universal relationship between low-energy AFM fluctuations and superconductivity, with the AFM fluctuation being the key parameter in the case of $\text{BaFe}_2(\text{As}_{1-x}\text{P}_x)_2$.

The authors acknowledge S. Yonezawa, Y. Maeno, and H. Ikeda for fruitful discussions. This work was partially supported by the Kyoto University LTM Center and Grant-in-Aids for Scientific Research (KAKENHI) (Grants No. JP15H05882, No. JP15H05884, No. JP15K21732, No. JP15H05745, No. JP17K14339, No. JP19K14657, No. JP19H04696, and No. JP19H05824).

-
- [1] J. Bardeen, L. N. Cooper, and J. R. Schrieffer, *Phys. Rev.* **108**, 1175 (1957).
- [2] T. Moriya and K. Ueda, *J. Phys. Soc. Jpn.* **63**, 1871 (1994).
- [3] Y. Nakai, T. Iye, S. Kitagawa, K. Ishida, S. Kasahara, T. Shibauchi, Y. Matsuda, H. Ikeda, and T. Terashima, *Phys. Rev. B* **87**, 174507 (2013).
- [4] J. L. Sarrao, E. D. Bauer, J. N. Mitchell, P. H. Tobash, and J. D. Thompson, *Physica C* **514**, 184 (2015).
- [5] Y. Nakai, T. Iye, S. Kitagawa, K. Ishida, H. Ikeda, S. Kasahara, H. Shishido, T. Shibauchi, Y. Matsuda, and T. Terashima, *Phys. Rev. Lett.* **105**, 107003 (2010).
- [6] K. Hashimoto, K. Cho, T. Shibauchi, S. Kasahara, Y. Mizukami, R. Katsumata, Y. Tsuruhara, T. Terashima, H. Ikeda, M. A. Tanatar, H. Kitano, N. Salovich, R. W. Giannetta, P. Walmsley, A. Carrington, R. Prozorov, and Y. Matsuda, *Science* **336**, 1554 (2012).
- [7] T. Moriya, Y. Takahashi, and K. Ueda, *J. Phys. Soc. Jpn.* **59**, 2905 (1990).
- [8] F. L. Ning, K. Ahilan, T. Imai, A. S. Sefat, M. A. McGuire, B. C. Sales, D. Mandrus, P. Cheng, B. Shen, and H.-H. Wen, *Phys. Rev. Lett.* **104**, 037001 (2010).
- [9] R. Zhou, Z. Li, J. Yang, D. Sun, C. Lin, and G.-q. Zheng, *Nat. Commun.* **4**, 2265 (2013).
- [10] G. F. Ji, J. S. Zhang, L. Ma, P. Fan, P. S. Wang, J. Dai, G. T. Tan, Y. Song, C. L. Zhang, P. Dai, B. Normand, and W. Yu, *Phys. Rev. Lett.* **111**, 107004 (2013).
- [11] M. Miyamoto, H. Mukuda, T. Kobayashi, M. Yashima, Y. Kitaoka, S. Miyasaka, and S. Tajima, *Phys. Rev. B* **92**, 125154 (2015).
- [12] L. E. Klintberg, S. K. Goh, S. Kasahara, Y. Nakai, K. Ishida, M. Sutherland, T. Shibauchi, Y. Matsuda, and T. Terashima, *J. Phys. Soc. Jpn.* **79**, 123706 (2010).
- [13] S. Hosoi, K. Matsuura, K. Ishida, H. Wang, Y. Mizukami, T. Watashige, S. Kasahara, Y. Matsuda, and T. Shibauchi, *Proc. Natl. Acad. Sci. USA* **113**, 8139 (2016).
- [14] J. P. Sun, K. Matsuura, G. Z. Ye, Y. Mizukami, M. Shimozawa, K. Matsubayashi, M. Yamashita, T. Watashige, S. Kasahara, Y. Matsuda, J. Q. Yan, B. C. Sales, Y. Uwatoko, J. G. Cheng, and T. Shibauchi, *Nat. Commun.* **7**, 12146 (2016).
- [15] S. Kawasaki, M. Yashima, Y. Mugino, H. Mukuda, Y. Kitaoka, H. Shishido, and Y. Ōnuki, *Phys. Rev. Lett.* **96**, 147001 (2006).
- [16] S. Kasahara, T. Shibauchi, K. Hashimoto, K. Ikada, S. Tonegawa, R. Okazaki, H. Shishido, H. Ikeda, H. Takeya, K. Hirata, T. Terashima, and Y. Matsuda, *Phys. Rev. B* **81**, 184519 (2010).
- [17] R. Mittal, S. K. Mishra, S. L. Chaplot, S. V. Ovsyannikov, E. Greenberg, D. M. Trots, L. Dubrovinsky, Y. Su, T. Brueckel, S. Matsuishi, H. Hosono, and G. Garbarino, *Phys. Rev. B* **83**, 054503 (2011).
- [18] P. L. Alireza, Y. T. C. Ko, J. Gillett, C. M. Petrone, J. M. Cole, G. G. Lonzarich, and S. E. Sebastian, *J. Phys.: Condens. Matter* **21**, 012208 (2009).
- [19] H. Kontani and S. Onari, *Phys. Rev. Lett.* **104**, 157001 (2010).
- [20] T. C. Kobayashi, H. Hidaka, H. Kotegawa, K. Fujiwara, and M. I. Eremets, *Rev. Sci. Instrum.* **78**, 023909 (2007).
- [21] K. Murata, K. Yokogawa, H. Yoshino, S. Klotz, P. Munsch, A. Irizawa, M. Nishiyama, K. Iizuka, T. Namba, T. Okada, Y. Shiraga, and S. Aoyama, *Rev. Sci. Instrum.* **79**, 085101 (2008).
- [22] A. Eiling and J. S. Schilling, *J. Phys. F: Met. Phys.* **11**, 623 (1981).
- [23] B. Bireckoven and J. Wittig, *J. Phys. E: Sci. Instrum.* **21**, 841 (1988).
- [24] See Supplemental Material at <http://link.aps.org/supplemental/10.1103/PhysRevB.100.060503> for the time dependence of recovery curves and for the θ dependence of T_c normalized by maximum T_c of each system in various iron-based superconductors, which includes Refs. [5,8–11,30].
- [25] K. Kitagawa, N. Katayama, K. Ohgushi, M. Yoshida, and M. Takigawa, *J. Phys. Soc. Jpn.* **77**, 114709 (2008).
- [26] S. Kitagawa, Y. Nakai, T. Iye, K. Ishida, Y. Kamihara, M. Hirano, and H. Hosono, *Phys. Rev. B* **81**, 212502 (2010).
- [27] Y. Nakai, S. Kitagawa, T. Iye, K. Ishida, Y. Kamihara, M. Hirano, and H. Hosono, *Phys. Rev. B* **85**, 134408 (2012).
- [28] M. Hirano, Y. Yamada, T. Saito, R. Nagashima, T. Konishi, T. Toriyama, Y. Ohta, H. Fukazawa, Y. Kohori, Y. Furukawa,

- K. Kihou, C.-H. Lee, A. Iyo, and H. Eisaki, *J. Phys. Soc. Jpn.* **81**, 054704 (2012).
- [29] Z. T. Zhang, D. Dmytriieva, S. Molatta, J. Wosnitza, S. Khim, S. Gass, A. U. B. Wolter, S. Wurmehl, H.-J. Grafe, and H. Kühne, *Phys. Rev. B* **97**, 115110 (2018).
- [30] T. Iye, Y. Nakai, S. Kitagawa, K. Ishida, S. Kasahara, T. Shibauchi, Y. Matsuda, and T. Terashima, *J. Phys. Soc. Jpn.* **81**, 033701 (2012).
- [31] A. P. Dioguardi, T. Kissikov, C. H. Lin, K. R. Shirer, M. M. Lawson, H.-J. Grafe, J.-H. Chu, I. R. Fisher, R. M. Fernandes, and N. J. Curro, *Phys. Rev. Lett.* **116**, 107202 (2016).